Computational and Theoretical Chemistry 1150 (2018): 110-120

DOI: https://doi.org/10.1016/j.comptc.2019.01.014

Insight into the optical properties of *meso*-pentafluorophenyl(PFP)-BODIPY: an attractive platform for functionalization of BODIPY dyes.

Martina De Vetta,[a,b] *and Inés Corral* [b,c,*]

[a] Institute of Theoretical Chemistry, Faculty of Chemistry, University of Vienna, Währinger Str. 17, A-1090 Wien, Austria

[b] Departamento de Química, Universidad Autónoma de Madrid, c/ Francisco Tomás y Valiente 7, 28049 Cantoblanco, Madrid, Spain

[c] IADCHEM. Institute for Advanced Research in Chemistry, Universidad Autónoma de Madrid, 28049 Cantoblanco, Madrid, Spain

* Corresponding Author:

email: ines.corral@uam.es

ABSTRACT

The pentafluorophenyl (PFP) moiety is an important and versatile substituent in the chemistry of BODIPYs, porphyrins and corroles. The widespread use of PFP *meso*-substituted compounds, as intermediates in the synthesis of more complex pyrrole derivatives, is the motivation behind this work, which investigates the optical properties of the *meso*-PFP-BODIPY from a theoretical point of view. From the panoply of computational tools available for this purpose, we have considered the CASPT2//CASSCF multiconfigurational protocol, and other monoreference methods, including time dependent density functional theory, TD-DFT, the second order approximate couple cluster, CC2, and the algebraic diagrammatic construction scheme of the polarization propagator in its second order, ADC(2), indicated for the description of medium size chromophores, with a complex electronic structure. We have identified ADC(2) as the most suited method for the characterization of the absorption properties of BODIPYs. Besides its computational efficiency and the small dependence shown towards the basis set flexibility, the black-box character of this method assures unbiased results. In general, all the methods evaluated show a good performance when compared with experimental results, especially if implicit solvent effects are taken into account, delivering errors which amount to 0.05 eV. Finally, we discuss the effect of the electron-withdrawing PFP substituent at the *meso*-position on the absorption and emission energies of the boron-dipyrromethene core. The comparison of the PFP-substituted and core BODIPY spectroscopic properties reveals that this substituent red-shifts both the absorption and the emission of the parent dye. On the one hand, the incorporation of this substituent was found to reduce the HOMO-LUMO gap, and on the other it induces a strong destabilization of the electronic ground state along the global coordinate leading

the system from the Franck-Condon region to the position of the first excited state, S_1, minimum, suggesting the proximity of the S_1/S_0 internal conversion funnel.

keywords: *meso*-substituted BODIPYs, ADC(2), CASPT2, absorption spectrum, emission.

1. Introduction

Boron-dipyrromethene (BODIPY) derivatives are extremely popular dyes. These chromophores are employed in many different fields ranging from material science [1–3] to biological applications such as bioimaging[4,5] or photodynamic therapy.[6–8] In fact, the possibility to rationally modulate the chemical, optical and photophysical properties of the parent BODIPY with appropriate substitution patterns,[9–11] is the origin of the great success of these compounds. The synthesis of novel derivatives, specifically designed for a target application, is therefore a very prolific field. Most commonly, BODIPY derivatives are synthetized via the one-pot two-step reaction schematically represented in Scheme 1, where the dipyrromethane precursor is first oxidized and then complexed using boron trifluoride etherate.[9,11]

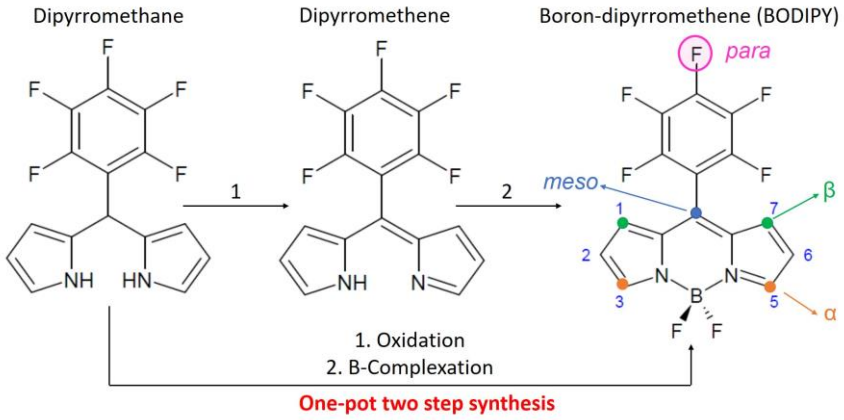

Scheme 1. Schematic one-pot two step synthesis of the *meso*-pentafluorophenyl BODIPY from its dipyrromethane precursor. The intermediate dipyrromethene compound is also reported. The characteristic *meso, α* and *β* positions on the core part of the BODIPY are highlighted in colors. The *para*- position on the aromatic substituent is also indicated.

It is remarkable that despite the synthesis of the first BODIPY was reported in 1968 [12], it took 40 additional years to synthesize for the first time the unsubstituted BODIPY core.[13,14] This has been ascribed to the high reactivity toward electrophiles and nucleophiles of the BODIPY scaffold where the electron density at the carbon atoms is polarized by the two nitrogen atoms of the pyrrolic units.[13] In addition, the dipyrromethene precursor is a highly unstable compound,[14] difficult to isolate unless appropriate substituents and synthetic strategies are adopted.[15–20] For example, the stabilization induced by the electron withdrawing PFP substituent allows the synthesis of α-monoalkoxy-substituted dipyrrins, [19] (recall atom labeling inherited from the BODIPY dipyrrin unit,[9] porphyrins and other porphyrinoids [21,22] in Scheme 1), from their dipyrrane precursor.

Interestingly, the *meso*-(PFP)-dipyrromethane precursor, shown in Scheme 1, represents a versatile starting material for the synthesis of *meso*-substituted BODIPYs but also of *trans*-A_2B_2-porphyrins[23] or *trans*-A_2B-corroles.[24] The electron-withdrawing PFP group at the *meso* position not only stabilizes the dipyrromethane scaffold but is also prone to react with a wide range of nucleophiles (e.g. amines, alcohols, thiols), selectively exchanging the fluorine atom at the *para*-position (recall Scheme 1).[25,26] This allows for the preparation of specific precursors, with the required chemical properties, for the final porphyrin or BODIPY derivative.[23] The nucleophilic substitution of dipyrromethane with polar amines and alcohols enables, for instance, the synthesis of porphyrinoids or BODIPYs with increased solubility in polar media intended for biomedical applications.[19,24] Besides the pre-functionalization of the dipyrromethane precursor, the post-functionalization of a PFP-substituted porphyrinoids or BODIPYs is also possible.[19,24,27] For example, the BODIPY reported in Scheme 1 can react with sodium azide leading to an azido functionalized derivative that is a potent unit to be used

in subsequent click-chemistry reactions.[23] Moreover, it is possible to combine α- and *para*-substitution to further tune the substitution pattern towards the desired application.[19,24,28]

Thus, thanks to its multiple functionalization possibilities the *meso*-(PFP)-BODIPY is an important precursor and building block for the design of more complex BODIPY derivatives. In addition, it contains - as basic chromophore - the dipyrromethene unit which is part of most porphyrinoid macrocycles like porphyrins, chlorins, corroles, hexaphyrins and even higher homologues. Thus, it is the aim of this work to investigate the optical properties of the *meso*-(PFP)-BODIPY, exploiting the insight that only theoretical approaches can provide.

To get the most out of this analysis we have predicted the absorption spectrum of this chromophore considering the effect of a solvent continuum or the configurational sampling of the most stable vibrational states of the electronic ground state. We have also assessed the performance of different computational protocols to discern which is the one providing the most satisfactory description of this family of dyes at the smallest computational cost. The scalability of the computational method of choice is in fact relevant for the screening of medium to large size BODIPYs derivatives with particular properties. [29]

The most popular computational methods for the description of the photophysical properties of dyes can be primarily divided in two categories; i.e. wave function based methods and density functional theory (DFT). Within the first category, further classifications can be made considering the single- or multi-configurational character of the reference wave function. Despite the high computational demand of these methods, the continuous development of both hardware and software technologies for quantum

mechanical calculations has allowed studying molecules of increasing size within this theoretical framework.[30–35]

One of the most popular multi-reference approaches for the characterization of the excited states of small to medium size dyes is the complete active space self-consistent field corrected with second-order perturbation theory CASPT2//CASSCF, that accounts for both static and dynamic correlation.[36] As for the single-reference methods, some of the most accepted are the second-order methods approximated coupled cluster singles and doubles CC2[37] and the algebraic diagrammatic construction scheme of the polarization propagator ADC(2)[38] that provide a balance between accuracy and computational cost. Finally, the time dependent derivation of DFT, TD-DFT, despite its limitations, is also highly appreciated for the computational efficacy demonstrated which allows to study relatively large molecular systems in contrast to the former methods and very particularly to the multireference approaches.[39,40]

The absorption spectrum is one of the properties most recurrently studied from a computational perspective in BODIPYs, as many of the processes behind the direct application of BODIPYs in different fields are initiated by light absorption.[30–32,41] Most of these simulations rely on the vertical approximation and consider the equilibrium geometry of the electronic Ground State (GS) as the most representative conformation of the molecule in the lowest vibrational state of its electronic fundamental state. Even though the calculated vertical transition energies at the ground state equilibrium geometry do not have a one to one correspondence with any vibrationally resolved band of the experimental absorption spectrum, these calculations still represent a straightforward way to interpret the optical properties of these systems, avoiding the calculation of Franck-Condon factors or the frequencies of the ground and excited states. [40,42–44]

A way to improve the simulation of the absorption spectrum is considering, besides the ground state equilibrium geometry, the contribution to the excitation process of other nuclear conformations participating in the ground state wave packet.[45,46] The simplest and probably the most reliable method for the sampling of the configurational/phase spaces to investigate both the absorption spectrum and the excited state dynamics is quantum sampling. Here, the ground state geometries of a system with N atoms are sampled according to their probability distribution in a given harmonic vibrational state. For the vibrational ground state, it is quite common to resort to an harmonic-oscillator Wigner distribution [47,48]. However, at room temperature (300 K) vibrational states other than the ground state, could also be populated, especially the ones with low vibrational frequencies ω. The following Wigner distribution P_W expression accounts for excited vibrational states populated under the harmonic approximation according to a Boltzmann distribution:

$$P_W^T(Q,P) = \frac{1}{(\pi\hbar)^{3N-6}} \prod_i^{3N-6} \alpha_i \exp\left(-\frac{2\alpha_i \mu_i \omega_i Q_i^2}{\hbar}\right) exp\left(\frac{2\alpha_i P_i^2}{\hbar \mu_i \omega_i}\right) \quad (1)$$

where the index i runs on the normal modes, μ accounts for their reduced masses and the term $\alpha_i = \tanh(\hbar\omega_i / 2k_B T)$ with k_B being the Boltzmann constant.[45]

Besides the level of theory or the computational protocol employed, the prediction of the absorption properties is also influenced by solute-environment interactions which can stabilize or destabilize a particular excited state provoking respectively a red- or blue-shift of the absorption/emission energies.[45,49–51] The use of implicit continuum solvation models, such as for instance the polarizable continuum model (PCM) [52] or the Conductor like screening model [53], allows accounting for the effect of the polarization of the solvent continuum and the screening of the partial charges of the solute in the excitation energies, either by considering the mutual influence of the

electrostatic fields of the solvent and the solute through an iterative approach, or by employing the scaled-conductor approximation. More sophisticated methods instead explicitly include the solvent at molecular detail in the calculation (explicit models), either using quantum mechanical or molecular mechanical [45,54–56] schemes. Finally, hybrid methods would combine explicit models for the first solvation shell(s) with the rest of the solvent being modelled implicitly.

Finally, our work, also discusses the effect of the PFP substituent placed at the *meso*-position on the predicted vertical absorption and emission energies and on the topography of the potential energy surfaces of the unsubstituted parent compound.

2. Computational Details

The GS geometry of the *meso*-substituted BODIPY was optimized employing density functional theory (DFT), with B3LYP[57] as exchange and correlation functional and the triple zeta polarized Pople basis set 6-311G**.[58]

The molecular absorption spectrum was computed convoluting the spectral lines of the first 10 excited states delivered by the different computational methods employed, except for the CASPT2/CASSCF multiconfigurational method where only 4 excited states have been calculated. For the second-order perturbation theory on complete active space self consistent field reference wave functions protocol (CASPT2//CASSSCF), able to account for both static and dynamic correlation, we considered the active space comprising 8 electrons in 7 orbitals (8,7), reported in Figure S1. For such calculation, we have employed a double zeta Pople 6-31G* basis set,[58] an IPEA shift of 0.25 a.u.[59,60] and a 0.1 a.u. level shift.[61] The RICD approximation[62] to compute the integrals was also adopted. This level of theory was also the one employed for the computation of the

vertical absorption energies of the 100 structures selected from the ensemble of 1000 geometries obtained by the harmonic oscillator vibrational sampling with a temperature dependent-Wigner distribution at 300 K, taking as input the harmonic frequency calculation undertaken at the same level of theory of the geometry optimization (DFT, B3LYP/6-311G*). The existence of low frequency modes, like BF_2 oscillation or the rotation of the *meso* substituent, make opportune the use of a temperature dependent-Wigner distribution, that would account for the population of excited vibrational states for these modes at room temperature.

The performance of the monoconfigurational second order methods, like the algebraic diagrammatic construction for the polarization propagator ADC(2)[38] and the singles and doubles coupled cluster approximation CC2,[37] with the aug-cc-pVDZ basis set[63] in the prediction of the absorption properties of this system was also assessed. For the ADC(2) method, the effect of the basis set size in the absorption energies was also evaluated and the aug-cc-pVDZ,[63] def-TZVP[64] and def-SVP[64] were considered. Finally, the monoconfigurational time dependent density functional theory (TD-DFT) spectra, considering (i) standard hybrid B3LYP,[57] PBE0,[65] functionals, (ii) the long-range corrected xc-functional, CAM-B3LYP,[66] (iii) the range separated functional wB97XD[67] which also accounts for dispersion corrections and (iv) the highly non-local functional M06-2X[68] were also analyzed. The basis set employed in all TD-DFT calculations was 6-311++G(d,p).[58] The TD-DFT results have been processed with the wave-function analysis software TheoDORE[69] and the so obtained Natural Transition Orbitals (NTOs) analyzed with the Jmol software package.[70] NTOs are derived from the transition density matrix and represent in a more compact manner the orbital nature of a particular electronic transition, especially when several configurations with a significant weight take part in the electronic excitation. In such orbital representation, the

occupied and virtual orbitals are the result of a linear combination of the canonical MOs that contribute to the configurations underlying the electronic excited state. [71,72] Solvent effects have been incorporated through the reoptimization of the equilibrium structure at DFT level with the polarizable continuum model (PCM)[52]. An epsilon value of 24.3 and a refracting index of 1.36 were used for the simulation of the spectra in ethanol. The effect of the polarization of the solvent on the ADC(2)/def-TZVP energies was instead simulated with the conductor like solvent model (COSMO) as implemented in Turbomole.[73] All the absorption spectra have been obtained by the convolution of the calculated spectral lines with Gaussian functions with full width at half maximum of 0.20 eV. Vertical energies at the FC region for the first 3 triplet excited states have also been computed at the ADC(2)/def-TZVP level of theory. Finally, we have also optimized the first singlet excited state in gas phase to compute vertical and adiabatic emission energies at the CC2 and ADC(2) level of theory with def-TZVP basis set. The CC2 and ADC(2) calculations were performed adopting the resolution of identity approximation for the calculation of four-center integrals.[74] All the DFT and TD-DFT calculations have been performed with the Gaussian09 software package.[75] The CC2 and ADC(2) calculation were carried out using the ricc2 module implemented in Turbomole-7.0[76] and the multi-reference calculations were undertaken with the Molcas 7[77] software.

3. Results

3.1. Benchmark of the computational protocol

The method that has been more intensively used in recent years to compute the optical properties of BODIPY derivatives is unequivocally TD-DFT.[40–44,78,79] Despite the accuracy of TD-DFT is known to be bound to the exchange and correlation functional

chosen, this method is, in fact, very convenient when BODIPYs carrying large substituents are studied, given its valuable scalability and computational efficiency.[32,41,79] As a first step in our study, we will discuss the absorption spectra predicted for *meso*-PFP-BODIPY by some of the most popular xc-functionals employed for BODIPYs.

From Figure 1a, two groups of spectra can be recognized, attending to the type of functional employed for the excited state calculation. The first group consists of the standard hybrid functionals B3LYP[57] and PBE0;[65] the second group instead, includes more sophisticated functionals, such as the long-range corrected CAM-B3LYP,[66] the range separated wB97XD[67] and the highly non-local M06-2X.[68]

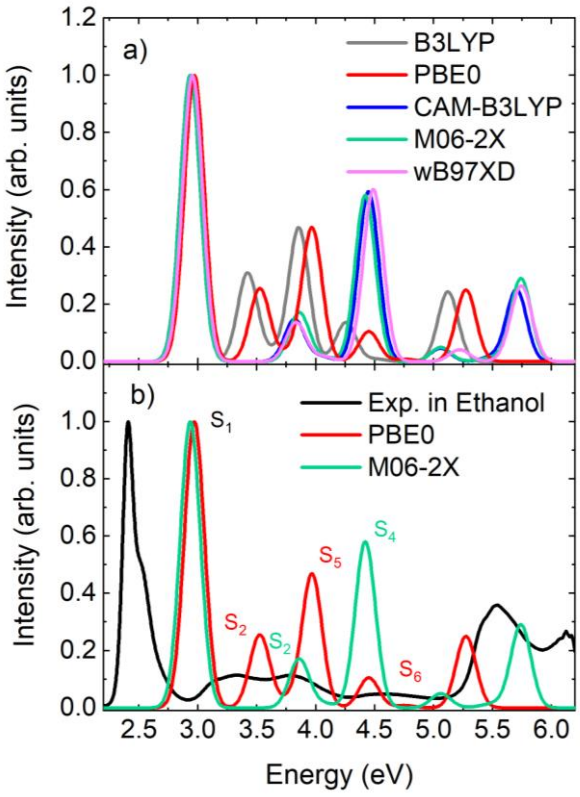

Figure 1. (a) *Meso*-PFP-BODIPY absorption spectra convoluting the first 10 electronic transitions computed at the TD-DFT level of theory with the xc functionals reported in the legend and 6-311+G(d,p) basis set. (b) Comparison of the experimental spectrum [80] with the theoretical spectra computed with the xc-functionals PBE0 and M06-2X. All the spectra are normalized.

Besides being strongly underestimated (0.55 eV), the energy of the main absorption band, characteristic of BODIPYs, does not show a strong dependence on the type of functional employed.[79] It is clear from Figure 1b, that the high-energy part of the absorption spectrum is, however, rather different depending on the class of functionals evaluated. Although the intensity of the second absorption band is overestimated by both classes of functionals, the M06-2X[68] functional, and in general all the functionals belonging to the second group, predict a specially high probability for the excitation at 4.42 eV, corresponding to the S_4 excited state. Table 1 also shows that the experimental second band convolutes three bright electronic transitions if PBE0[65] is used, whereas only two bright excitations are calculated in this energy range by the M06-2X[68] xc-functional.

Table 1. Characterization of the first two bands of the absorption spectra at the TD-DFT level of theory with the PBE0 and the M06-2X functionals.

PBE0					
	Exc.	E (eV)	*f*	Config.	Weight
1st Band	S_1	2.97	0.3700	H L	92.2%
				H-1 L	7.8%
2nd Band	S_2	3.53	0.0941	H-1 L	91.6%
				H L	7.9%
	S_5	3.97	0.1725	H-4 L	97.3%
	S_6	4.45	0.0389	H L+1	99.1%
M06-2X					
	Exc.	E (eV)	*f*	Config.	Weight
1st Band	S_1	2.94	0.4279	H L	96.7%
				H-1 L	2.8%
2nd Band	S_2	3.86	0.0941	H-1 L	96.1%
				H L	3.1%

S_4	4.42	0.1725	H-4	L	96.1%

Also interestingly, despite both functionals predict the same character for the S_1 and S_2 transitions, with orbitals localized on the BODIPY core, and similar energies for the first transition, PBE0 calculates the S_2 excitation to be 0.33 eV more stable than M06-2X. Such a difference can be understood examining the configuration weights in the wave function or more visually by inspecting the natural transition orbital (NTO) pairs corresponding to this excitation for the two functionals reported in Figure 2. Consistently with the character of the S_2 wavefunction (recall Table 1), the comparison between the PBE0 and M06-2X occupied NTO and canonical orbitals (See Figure 2 and S2) reveals the more important contribution of the HOMO orbital in the S_2 transition for the former than for the latter, and thus would possibly explain the red shift of the band.

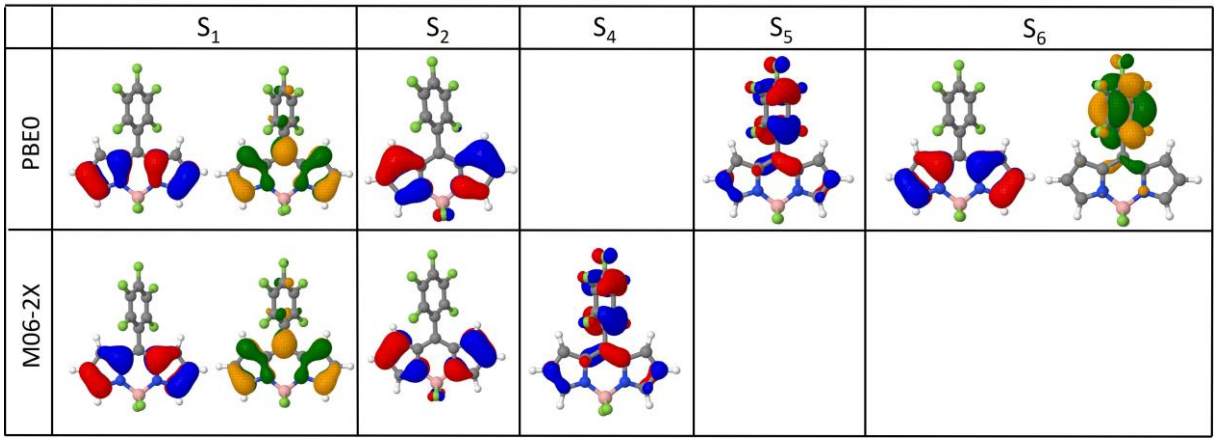

Figure 2. NTOs for the bright states of the first and second absorption band computed with PBE0 and M06-2X functionals. The phases of the occupied orbitals are reported in blue/red while for the virtual ones yellow/green colours have been used. For the S_1, S_2, S_4 and S_5 the virtual orbital is the same and is reported only in the S_1 panel for clarity.

The S_5 and S_6 excitations in PBE0 and the S_4 transition with M06-2X in contrast have a markedly charge transfer (CT) character. Whilst the PBE0 S_5 and M06-2X S_4 states consist of an electron transfer from the aromatic ring of the *meso* substituent to the BODIPY core; the reverse process if observed for the PBE0 S_6 electronic transition, where an electron is promoted from the BODIPY core to the substituent. Given the nature of these transitions, it is not surprising that the two groups of functionals predict different results for the high-energy part of the spectrum. In fact, it is well known that standard hybrid functionals, such as PBE0, strongly underestimate the energy of CT excitations, due to their impossibility to correctly reproduce the 1/r (with r denoting the nucleus-electron distance) behavior [81,82] and the missing derivative discontinuities [83]. This problem is, however, partially circumvented upon introducing long range corrections or when resorting to more advanced functionals like M06-2X which together with other Minnesota functionals, such as M05-2X and M06-HF were found to perform reasonably for charge transfer transitions[68]. In fact, the M06-2X functional is able to qualitatively reproduce the shape of the high energy region of the experimental absorption as showed in Figure 1b, despite the 0.5 eV shift to higher energies and the differences in the relative intensities of these bands predicted by theory. The standard hybrid functional PBE0, in turn, underestimates the energy of the S_2 excited state, lying this band too close in energy to the main absorption feature (compare the ΔE_{S1-S2}=0.56 eV in PBE0 vs. 0.92 eV in M06-2X and 0.91 in the experiment).

Figure 3 compares the absorption spectrum calculated with TD-M06-2X with that calculated with the other two monoconfigurational methods included in our survey, the popular second-order monoconfigurational methods, CC2 and ADC(2). We have also considered the effect in the shape and energy of the absorption spectrum of static correlation through the multiconfigurational method CASSCF, corrected via its second order

perturbation variant MS-CASPT2, through which dynamical correlation is as well introduced.

The major drawback of the CASPT2/CASSCF method is the definition of a computationally affordable active space, which at the same time provides an accurate description of the electronic structure of medium/large molecules and/or of a certain complexity. And this problem becomes even more crucial if excited state optimizations are required.

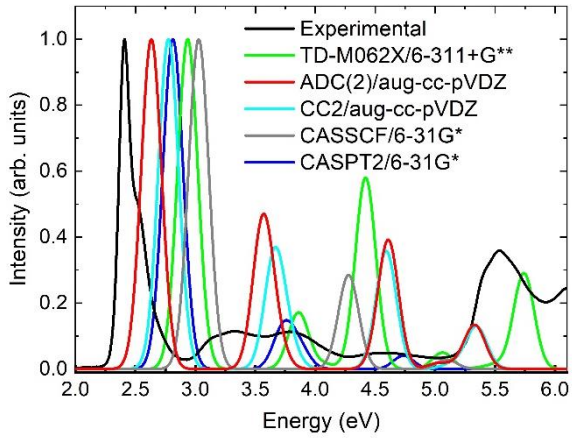

Figure 3. Comparison of the performance of several mono- and multiconfigurational methods (reported in the legend) taking as a reference the experimental spectrum recorded in ethanol. [80]

The examination of Figure 3 reveals that the MS-CASPT2 spectrum, normally taken as a benchmark,[32] does not provide the best agreement with the experimental reference. In fact, the CASPT2/CASSCF first band, which shows a remarkable overlap with CC2, deviates by 0.4 eV to higher energies with respect to the experimental value lying at 2.41 eV. The reduced size of the active space employed for the prediction of the MS-CASPT2 spectrum, not comprising the full valence π space, is actually at the origin of the discrepancy of this method with the experimental results. In fact, enlarging the active space

to (12,11) so that it includes all the π orbitals of the core part of the BODIPY[84] results in a better comparison with the experiment. The main absorption feature S_1 calculated with the larger active space appears at 2.64 eV and 2.49 eV in the CASSCF and MS-CASPT2 spectra, respectively, reducing the error with respect the experimental value to 0.23 and 0.08 eV. Despite this reduction in the errors, the active space does not yet contain all the π orbitals of the *meso*-PFP-BODIPY and, for example, there is probably still room for the improvement in the description of the CT excitations. Moreover, gradient calculation using the extended (12,11) active space implies a considerable increase in the computational cost of the calculations and for this reason in the following only the calculations performed with the smaller (8,7) AS will be discussed. Besides that, it should also be noticed that the spectra represented in Figure 3 rely on the vertical approximation and neglect the effect of the solvent.

The most accurate prediction (leaving aside the CASPT2 calculation on CASSCF(12,11) wave functions), at least in what refers to the first absorption band, is provided by the ADC(2) method, which calculates the S_1 absorption of the *meso*-PFP-BODIPY at 2.63 eV with an error of 0.22 eV relative to the experimental value. This agreement is, however, not extensive to the prediction of the relative intensities of the transitions. In fact, the preferred method for the prediction of excitation energies very importantly overestimates the oscillator strengths beyond the S_1. Despite the shift of the CASPT2 absorption bands and the reduced number of electronic excited states considered in the calculation, the CASPT2//CASSCF is the method among all the protocols considered which better reproduces the relative intensities of the first absorption band with the high-energy region of the spectrum.

Both ADC(2) and MS-CASPT2 predict the S_1 excitation to be mainly due to a HOMO-LUMO transition (with 83.3% and 71.1% configuration weights, respectively) with the

second most important configuration being HOMO-1-LUMO (with weights of 12.2% and 11% for ADC(2) and CASPT2). The second most stable bright state S_2 presents a complementary character relative to the S_1: for ADC(2), the main contribution arises from the HOMO-1-LUMO transition with a weight of 82.3% followed by a 13.1% contribution from the HOMO-LUMO transition. In the case of the multiconfigurational method CASPT2, the HOMO-1-LUMO transition has a weight of 56.5% in the total wavefunction, with a 10.7% contribution from the HOMO-LUMO transition and an additional contribution (19%) from a double excitation involving the HOMO-2, the HOMO and the LUMO orbitals. The higher lying CT excitation is also predicted at the ADC(2) level of theory to be rather monoconfigurational, with the HOMO-4-LUMO transition contributing most to the wavefunction (91.7%). However, such an excitation was not computed at the CASPT2 level of theory for which only four excited states have been considered. The CC2 method predicts almost the same wavefunctions as ADC(2), with configurational weights that differ at most by 2%.

For the purpose of improving our CASPT2 description of the *meso*-PFP-BODIPY absorption spectrum and, thus, to achieve an accurate assignment of the experimental absorption bands, we have abandoned the vertical approximation and calculated the semi-classical spectrum at the MS-CASPT2 level of theory. Despite the blue-shift of the absorption energies calculated by CASPT2, Figure 4a shows a very reasonable agreement between the CASPT2 and the experimental spectrum in the energy range comprised between 1.75 eV and 5 eV, covered by the first four electronic states considered in the calculation. From the spectrum decomposition, we observe that the first experimental absorption band fully arises from the first excited state S_1, which is the characteristic HOMO-LUMO transition of the BODIPY family. The second experimental band, which presents two maxima at 3.33 and 3.80 eV, corresponds to the electronic excited states S_2

and S_3. The S_2 excited state main contribution arises from the HOMO-1-LUMO transition with minor contributions from HOMO-LUMO, HOMO-2-LUMO and a double excitation involving the promotion of two electrons from the HOMO-2 and the HOMO to the LUMO orbital. Finally, the S_3 state presents mainly a HOMO-2-LUMO character, with smaller contributions from the HOMO-1-LUMO and the HOMO-LUMO transitions. Also for this state, a double excitation contributes to the overall wavefunction, corresponding to the promotion of two electrons from the HOMO and the HOMO-1 to the LUMO.

This decomposition actually coincides with the assignment provided by the FC ADC(2) and CASPT2 spectra.

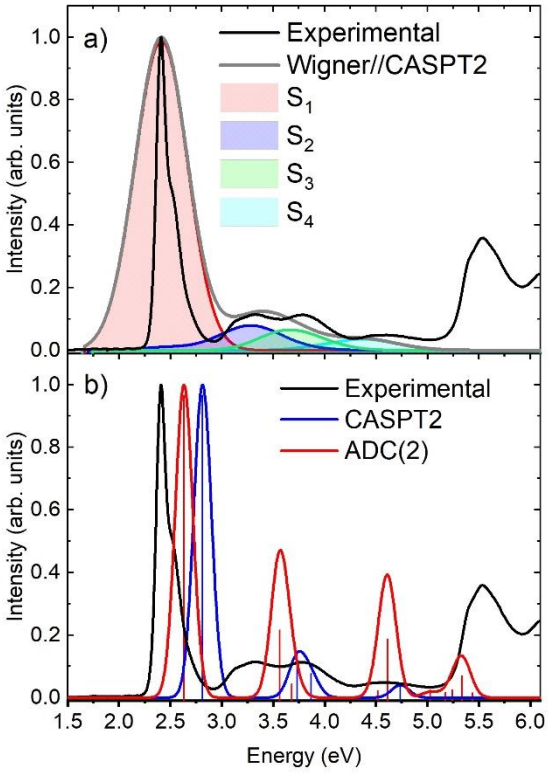

Figure 4. Semiclassical MS-CASPT2/6-31G* absorption spectrum (shifted by -0.36 eV) superimposed to the decomposition of the different excited state contributions and the experimental spectrum [80] (a) and comparison of the FC line spectra calculated at the MS-CASPT2/6-31G* and ADC(2)/aug-cc-pVDZ levels of theory with the corresponding spectral lines (b).

From the comparison of the semiclassical spectrum, (Figure 4a) obtained by the Wigner distribution of the most stable vibrational states of the electronic ground state, and the FC spectrum, (Figure 4b) based on the sole geometry of the GS minimum, we observe that besides the natural broadening of the absorption bands arising from the consideration of geometries other than the FC, the center of absorption bands also experiences a small red-shift (0.05 eV).

Now that it has been established the superiority of the ADC(2) method in the description of the optical properties of *meso*-substituted BODIPYs, we would like to consider the effect of additional factors, e.g. basis set and solvation, on the quality of the theoretical spectrum. The use of a monoreferential method is advantageous because of its black box nature: the results are not influenced by the number of excited states calculated or by the active space selected. Such features are particularly valuable for the search of BODIPY derivatives with specific photophysical properties, where the effect of a large number of substituents on the optical and photophyical properties of the dye has to be evaluated.

So far the assignment of the absorption spectrum of *meso*-PFP-BODIPY calculated with the ADC(2) method combined with an augmented correlation consistent double zeta basis set (aug-cc-pVDZ) has been discussed. In the following, we will report on the influence of the flexibility of the basis set on the results. Our survey includes the Karlsruhe basis def-SVP and def-TZVP, which similarly to the Dunning basis, include diffuse functions.

As shown in Figure 5a, the effect of the basis set on the absorption spectrum of the BODIPY derivative is not significant. For the first main absorption band of BODIPYs, there is 0.07 eV difference between the energies calculated with the def-SVP and the def-TZVP basis sets. As for the high-energy region of the spectrum, larger differences (0.1 eV)

between the energies calculated with the three basis sets considered in our survey were identified.

As expected, the most flexible basis set, def-TZVP, delivers the smallest error for the S_1 absorption, and calculates the first transition 0.21 eV blue-shifted with respect to the experimental curve recorded in ethanol. This energy difference is reduced to only 0.05 eV, as showed by Figure 5b, when solvent effects are introduced via the implicit conductor like screening solvation model (COSMO). The effect of the solvent, though, is not homogeneous for all the absorption bands. The red-shift registered for the first absorption band, which amounts to 0.16 eV, is much more pronounced than for the second band where the energy difference between the gas phase and solvated spectra is only 0.03 eV, consistently with the dipole moments of these transitions, (see Table S1). Moreover, there is a redistribution of the absorption intensity between the second (S_2 transition) and third (S_5 transition) absorption bands. Upon solvent inclusion, the S_5 excited state, which has a CT character, overpasses in intensity the local $\pi\pi^*$ S_2 excitation, reversing the gas phase probability of these two transitions. Also consistent with its lower polarity compared to the GS (recall Table S1), the third band (S_5 transitions) also experiments a significant red-shift compared to the gas phase situation, which amounts in this case to 0.35 eV. The differences between the gas phase and solution spectra in the high-energy region cannot be exclusively ascribed to the effect of the mutual influence of the polarized solvent and excited solute, but also to a change in the electronic excitation. In fact, whilst in the gas phase the occupied orbitals involved in the transitions and corresponding to the second and third excited states are confined on the core part, these orbitals are more delocalized in solution.

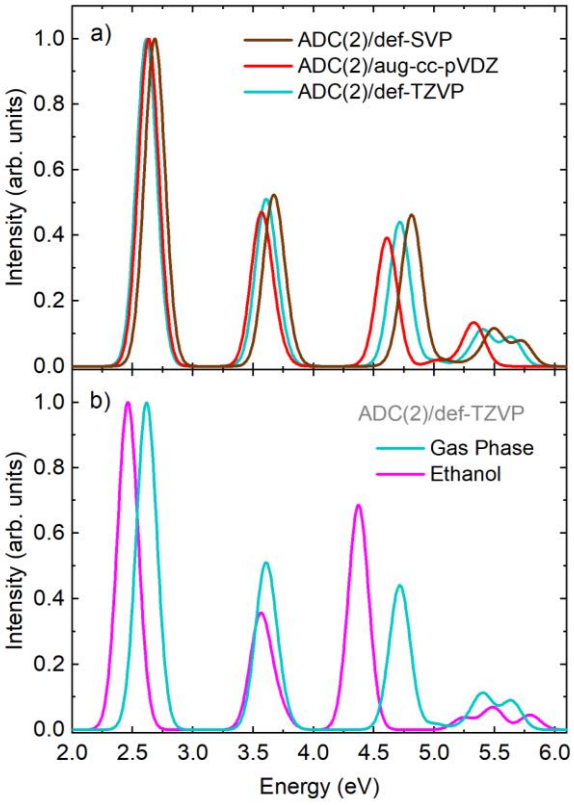

Figure 5. Effect of the basis set size (a) and of ethanol solvent (COSMO implicit solvation model) (b) on the absorption spectrum of the *meso*-PFP-BODIPY. The level of theory employed for these simulations is indicated in the legend.

3.2 Effect of the *meso*-PFP group in the absorption spectrum

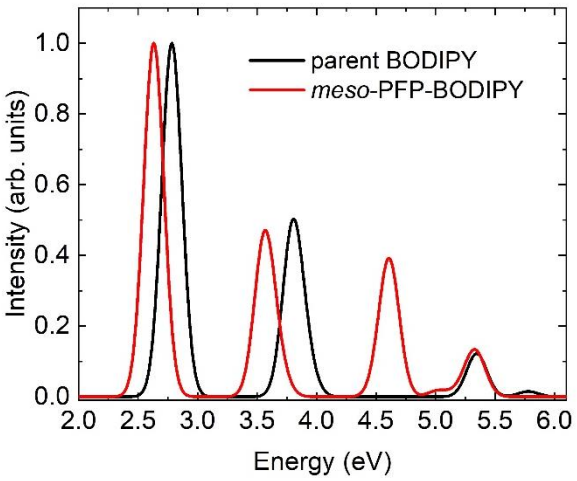

Figure 6. Comparison of the computed absorption spectra of the *meso*-PFP-BODIPY and the parent compound at the ADC(2)/aug-cc-pVDZ level of theory. [84]

Figure 6 collects the absorption spectra calculated for the core and the *meso*-PFP substituted BODIPYs. The functionalization at the *meso* position with the aromatic substituent introduces a red shift (0.15 eV) in the first absorption bands of the spectrum of the BODIPY core, even though this transition arises from the promotion of electrons between orbitals confined on the core part of the BODIPY.

Such effect has been already discussed in other works analyzing *meso*-substituted BODIPYs [30,85–87] and has been ascribed to the stabilization of the LUMO orbital, which is partially localized on the *meso* carbon, induced by electron-withdrawing groups such as the PFP (see Figure 2). This would reduce the HOMO-LUMO gap, decreasing the excitation energy corresponding to such electronic transition.

The second band is also shifted (0.23 eV) towards lower energies in the *meso*-substituted BODIPY compared to the parent BODIPY absorption spectrum, whilst the transition peaking around 5.3 eV does not seem to be affected by the substitution at the *meso* position. Interestingly, a new feature, not present in the core BODIPY absorption spectrum, arises for the *meso*-substituted compound. This transition (S_5) has actually its origin in the CT excitation discussed in the previous section, responsible for the transfer of electron density from a π orbital localized on the substituent to the core of the dye.

In many cases, the effect of the substituents on the electronic excited states of a particular multiplicity cannot be extrapolated to excited states of different spin.[8] In the following, we will compare the energies and character of the lowest lying triplet excited states of the parent compound and its *meso* substituted derivative.

Table 2. FC relative energies (in eV) calculated at the ADC(2)/def-TZVP level of theory of the first spectroscopic state and the three lowest lying triplet excited states of parent BODIPY and the *meso*-PFP-BODIPY. The singlet-triplet (S_1-T_n) energy gaps are reported in eV in parenthesis.

	parent BODIPY	*meso*-PFP-BODIPY
S_1	2.78 eV	2.62 eV
T_1 ($\pi\pi^*$)	1.92 eV (0.72 eV)	1.82 eV (0.79 eV)
T_2 ($\pi\pi^*$)	3.11 eV (0.47 eV)	2.93 eV (0.32 eV)
T_3 ($\pi\pi^*$)	3.31 eV (0.67 eV)	3.16 eV (0.55 eV)

From the examination of Table 2, we observe that the *meso* substituent stabilizes by 0.1- 0.2 eV both the lowest lying singlet and triplet states compared to the parent compound. Thus, the calculated S_1-T_n energy gaps (ΔE_{S-T}) are rather similar for the 2 compounds. Singlet-triplet intersystem crossing is of interest for several BODIPYs applications that exploit the population of the triplet excited states [8,88–90] of the dye, e.g. photodynamic therapy,[6,7] triplet-triplet annihilation conversion,[91–93] etc. Similarly to what found for the parent compound, the second triplet state T_2 of the *meso*-PFP-BODIPY is the closest triplet to the S_1. The proximity of these electronic states at the FC region, however, does not grant the existence of real singlet triplet energetically accessible funnels between these electronic states in other regions of the PES.

For the parent BODIPY compound, the S_1/T_2 crossing is accidentally the most plausible funnel for the transfer of population to the triplet manifold from the S_1 minimum, where the population is redirected following electronic excitation and which is responsible for the fluorescence properties of the dye. [84] But it cannot be excluded that the *meso* substituent sculpts the parent BODIPY excited state potential energy surface activating other funnels along the relaxation pathway of the S_1.

Nevertheless, the coupling between the singlet and triplet states is expected to be small because of the character of the excitations from the two multiplicities, as it was found for

the parent compound. According to the El-Sayed rules [94], in fact, states with same character, like this case, would show small spin orbit coupling values and therefore small probabilities of population transfer to the triplet manifold.

According to our ADC(2)/def-TZVP calculations, the S_1 minimum of PFP-substituted BODIPY, would be located 2.38 eV above the ground state equilibrium structure, that is 0.25 eV below the FC value. The opposite behavior is, however, observed along the S_1 relaxation coordinate for the S_0, leading to a S_1 vertical emission energy, which amounts to 1.92 eV. This value is significantly smaller than the vertical emissions predicted by the monoreferential second-order method CC2, and the multiconfigurational methods CASSCF and CASPT2 with the 6-31G* basis set which amount to 2.16 eV, 2.58 and 2.52 eV, respectively. The adiabatic S_{1min}-S_0 energies for these methods are instead 2.52, 2.83 and 2.98 eV for CC2, CASSCF and MS-CASPT2, respectively.

According to the calculated S_1-T_n energy gaps at the position of the S_1 minimum, the triplet excited states to be most likely populated from the spectroscopic state minimum are the T_1 and T_2 ($\Delta E_{S\text{-}T}$ = 0.38 eV).

For the parent compound, the minimum of the spectroscopic state at the ADC(2)/def-TZVP level of theory lies 2.55 eV relative to the GS minimum. Thus, this corresponds to an energetic stabilization of 0.23 eV for S_1 excited state relative to the FC region, similarly to the *meso*-substituted compound. The destabilization of the fundamental state S_0 in the parent compound along the S_1 relaxation coordinate is, however, less pronounced resulting in a greater vertical emission energy of 2.32 eV. As for the S_1-T_n energy gaps, the S_1-T_1 energy gap calculated for the parent compound is 0.6 eV, [84] which is larger than the one found for the *meso*-substituted BODIPY (0.38 eV). The T_2 state is the closest triplet to the S_1 minimum in the parent compound with an energy gap of 0.4 eV.[84] The comparison of

the vertical absorption and emission energies for the two BODIPYs discussed in this Section is summarized in Scheme 2.

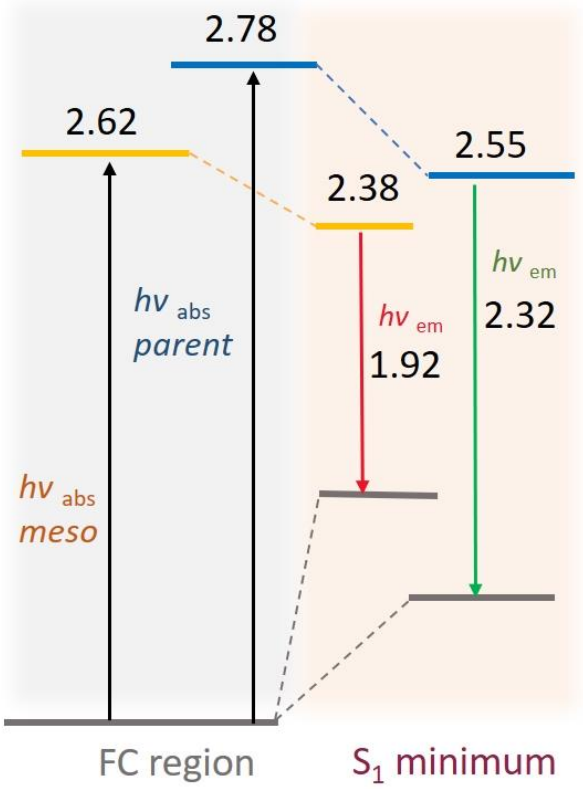

Scheme 2. Scheme collecting the vertical absorption and emission energies of the *meso*-substituted and the parent BODIPY.

The greater destabilization of the GS along the S_1 relaxation coordinate registered for the *meso*-substituted derivative, suggests the proximity of a radiationless deactivation funnel S_1/S_0. The most probable deactivation mechanism, and specifically the competition between fluorescence and internal conversion, has been extensively discussed for *meso*-substituted BODIPYs in the literature. [34,35,86,87,95] Substituents that link through an sp^2 carbon to the *meso* position of the BODIPY scaffold, e.g. and aromatic ring, were found to quench the

fluorescence quantum yield of these dyes, and thus to favor the deactivation through internal conversion processes.[34,86,87]

4. Conclusions

In this work we have explored the optical properties of the *meso*-PFP-BODIPY, as a representative of other *meso*-PFP compounds employed as intermediates in the synthesis of biologically relevant macrocycles such as *trans*-A_2B_2-porphyrins. The absorption spectrum of this compound was computed in the framework of the popular TD-DFT formalism using two different classes of xc-functionals. From our analysis, we conclude that the accuracy of the TD-DFT absorption energies is bound to the character of the excited state and thus depend very much on the electronic structure of the compound under scrutiny. In this work, we have also assessed the performance of other methods in the prediction of the photophysical properties of this species. Namely, we have included the CC2, ADC(2), CASSCF and MS-CASPT2 in our survey. Interestingly, we have found that ADC(2), besides having the advantage of being a black-box method, also predicts more accurate energies than CASPT2, in particular when reduced active spaces have to be considered due to the complexity of the systems. Switching from the vertical to a semi-classical approximation within the CASPT2 framework, allows the natural broadening of the absorption bands simultaneous to the slight red shift of the absorption band centers, improving this way the agreement with the experiment.

An improvement of the agreement between the most accurate ADC(2) spectrum with the experiment is also achieved after implicitly introducing solvent-solute interactions, whilst the flexibility of the basis set size does not seem to affect the quality of the spectrum in a significant way.

From the comparison of the spectra of the core BODIPY and the BODIPY derivative, we conclude that PFP substituent at the *meso* position red shifts the lowest energy absorption bands by 0.15-0.2 eV, due to the stabilization of the LUMO orbital. Also interestingly, the calculated S_1-T_1 and S_1-T_2 energy gaps at the position of the S_1 minimum in the *meso*-PFP substituted BODIPY are considerably smaller than the ones calculated for the unsubstituted derivative.

Moreover, the destabilization of the S_0 at the position of the S_1 minimum is greater in the substituted derivative, suggesting the proximity of the S_1/S_0 conical intersection. The potential accessibility of the S_1/S_0 and the small couplings expected between the singlet and triplet states because of their similar character according to the El-Sayed rules [94] is consistent with the quenching of the fluorescence and the enhancement of internal conversion processes observed in BODIPY derivatives substituted at the *meso* position with unsaturated or aromatic groups.

Acknowledgments

The authors would like to thank Dr. Arno Wiehe and Dorika Steen from Biolitec research GmbH for their valuable discussions and for providing the experimental absorption spectrum of the *meso*-PFP-BODIPY. This work has been supported by the Project CTQ2015-63997-C2 of the Ministerio de Economía y Competitividad of Spain. I.C. gratefully acknowledges the "Ramón y Cajal" program of the Ministerio de Economía y Competitividad of Spain. M.D.V. thanks the Marie Curie Actions, within the Innovative Training Network-European Join Doctorate in Theoretical Chemistry and Computational Modelling TCCM-ITN-EJD-642294, for financial support. Computational time from the Centro de Computación Científica (CCC) of Universidad Autónoma de Madrid is also gratefully acknowledged.

References

[1] H. Yeo, K. Tanaka, Y. Chujo, Effective light-harvesting antennae based on BODIPY-tethered cardo polyfluorenes via rapid energy transferring and low concentration quenching, Macromolecules. 46 (2013) 2599–2605. doi:10.1021/ma400015d.

[2] S. Debnath, S. Singh, A. Bedi, K. Krishnamoorthy, S.S. Zade, Synthesis, Optoelectronic, and Transistor Properties of BODIPY- and Cyclopenta[*c*]thiophene-Containing π-Conjugated Copolymers, J. Phys. Chem. C. 119 (2015) 15859–15867. doi:10.1021/acs.jpcc.5b02743.

[3] J.J. Chen, S.M. Conron, P. Erwin, M. Dimitriou, K. McAlahney, M.E. Thompson, High-efficiency BODIPY-based organic photovoltaics, ACS Appl. Mater. Interfaces. 7 (2015) 662–669. doi:10.1021/am506874k.

[4] A.M. Courtis, S.A. Santos, Y. Guan, J.A. Hendricks, B. Ghosh, D.M. Szantai-Kis, S.A. Reis, J. V. Shah, R. Mazitschek, Monoalkoxy BODIPYs-A fluorophore class for bioimaging, Bioconjug. Chem. 25 (2014) 1043–1051. doi:10.1021/bc400575w.

[5] S. Kolemen, E.U. Akkaya, Reaction-based BODIPY probes for selective bio-imaging, Coord. Chem. Rev. 354 (2018) 121–134. doi:10.1016/j.ccr.2017.06.021.

[6] A. Kamkaew, S.H. Lim, H.B. Lee, L.V. Kiew, L.Y. Chung, K. Burgess, BODIPY dyes in photodynamic therapy., Chem. Soc. Rev. 42 (2013) 77–88. doi:10.1039/c2cs35216h.

[7] S.G. Awuah, Y. You, Boron dipyrromethene (BODIPY)-based photosensitizers for photodynamic therapy, RSC Adv. 2 (2012) 11169. doi:10.1039/c2ra21404k.

[8] J. Zhao, K. Xu, W. Yang, Z. Wang, F. Zhong, The triplet excited state of Bodipy:

formation, modulation and application, Chem Soc Rev. 44 (2015) 8904–8939. doi:10.1039/c5cs00364d.

[9] A. Loudet, K. Burgess, BODIPY Dyes and Their Derivatives: Syntheses and Spectroscopic Properties, Chem. Rev. 107 (2007) 4891–4932. doi:doi:10.1021/cr078381n.

[10] J. Bañuelos, BODIPY Dye, the Most Versatile Fluorophore Ever?, Chem. Rec. 16 (2016) 335–48. doi:10.1002/tcr.201500238.

[11] G. Ulrich, R. Ziessel, A. Harriman, The chemistry of fluorescent bodipy dyes: Versatility unsurpassed, Angew. Chemie - Int. Ed. 47 (2008) 1184–1201. doi:10.1002/anie.200702070.

[12] A. Treibs, F.-H. Kreuzer, Difluorboryl-Komplexe von Di- und Tripyrrylmethenen, Justus Liebigs Ann. Chem. 718 (1968) 208–223. doi:10.1002/jlac.19687180119.

[13] A. Schmitt, B. Hinkeldey, M. Wild, G. Jung, Synthesis of the core compound of the BODIPY dye class: 4,4'-difluoro-4-bora-(3a,4a)-diaza-s-indacene, J. Fluoresc. 19 (2009) 755–758. doi:10.1007/s10895-008-0446-7.

[14] I.J. Arroyo, R. Hu, G. Merino, B.Z. Tang, E. Peña-Cabrera, The smallest and one of the brightest. Efficient preparation and optical description of the parent borondipyrromethene system, J. Org. Chem. 74 (2009) 5719–5722. doi:10.1021/jo901014w.

[15] S.R. Halper, J.R. Stork, S.M. Cohen, Preparation and characterization of asymmetric α-alkoxy dipyrrin ligands and their metal complexes, Dalt. Trans. 10 (2007) 1067–1074. doi:10.1039/b615801c.

[16] J.Y. Shin, D. Dolphin, Synthesis of a class of 5-((5-(pyrrol-2-yl-methylene)-pyrrol-2-

yl) methylene)furan-2-ones and the formation of a furanone dipyrrin imino ether, New J. Chem. 35 (2011) 2483–2487. doi:10.1039/c1nj20415g.

[17] J.Y. Shin, B.O. Patrick, D. Dolphin, Facile synthesis of dicyanovinyl-di(meso-aryl)dipyrromethenes via a dipyrromethene-DDQ adduct, Org. Biomol. Chem. 7 (2009) 2032–2035. doi:10.1039/b904446a.

[18] R.K. Gupta, R. Pandey, S. Sharma, D.S. Pandey, Synthesis of electroactive multinuclear dipyrrinato complexes and Fe(iii) assisted formation of α-alkoxy substituted 5-ferrocenyldipyrromethenes, Dalt. Trans. 41 (2012) 8556–8566. doi:10.1039/c2dt30212h.

[19] C.S. Gutsche, B.F. Hohlfeld, K.J. Flanagan, M.O. Senge, N. Kulak, A. Wiehe, Sequential Nucleophilic Substitution of the α-Pyrrole and p-Aryl Positions of meso-Pentafluorophenyl-Substituted BODIPYs, European J. Org. Chem. 2017 (2017) 3187–3196. doi:10.1002/ejoc.201700264.

[20] C.S. Gutsche, S. Gräfe, B. Gitter, K.J. Flanagan, M.O. Senge, N. Kulak, A. Wiehe, Pre-/post-functionalization in dipyrrin metal complexes – antitumor and antibacterial activity of their glycosylated derivatives, Dalt. Trans. (2018). doi:10.1039/C8DT03059F.

[21] G. Moss, NOMENCLATURE OF TETRAPYRROLES, Pure Appl. Chem. 59 (1987) 779–832. doi:10.1351/pac198759060779.

[22] T. Tanaka, A. Osuka, Chemistry of meso-Aryl-Substituted Expanded Porphyrins: Aromaticity and Molecular Twist, Chem. Rev. 117 (2017) 2584–2640. doi:10.1021/acs.chemrev.6b00371.

[23] H.R.A. Golf, H.U. Reissig, A. Wiehe, Nucleophilic substitution on

(Pentafluorophenyl)dipyrromethane: A new route to building blocks for functionalized BODIPYs and tetrapyrroles, Org. Lett. 17 (2015) 982–985. doi:10.1021/acs.orglett.5b00082.

[24] C.S. Gutsche, M. Ortwerth, S. Gräfe, K.J. Flanagan, M.O. Senge, H.U. Reissig, N. Kulak, A. Wiehe, Nucleophilic Aromatic Substitution on Pentafluorophenyl-Substituted Dipyrranes and Tetrapyrroles as a Route to Multifunctionalized Chromophores for Potential Application in Photodynamic Therapy, Chem. - A Eur. J. 22 (2016) 13953–13964. doi:10.1002/chem.201601857.

[25] N.V.S.D.K. Bhupathiraju, W. Rizvi, J.D. Batteas, C.M. Drain, Fluorinated porphyrinoids as efficient platforms for new photonic materials, sensors, and therapeutics, Org. Biomol. Chem. 14 (2015) 389–408. doi:10.1039/c5ob01839k.

[26] T. Goslinski, J. Piskorz, Fluorinated porphyrinoids and their biomedical applications, J. Photochem. Photobiol. C Photochem. Rev. 12 (2011) 304–321. doi:10.1016/j.jphotochemrev.2011.09.005.

[27] A. Aggarwal, S. Thompson, S. Singh, B. Newton, A. Moore, R. Gao, X. Gu, S. Mukherjee, C.M. Drain, Photophysics of glycosylated derivatives of a chlorin, isobacteriochlorin and bacteriochlorin for photodynamic theragnostics: Discovery of a two-photon-absorbing photosensitizer, Photochem. Photobiol. 90 (2014) 419–430. doi:10.1111/php.12179.

[28] N. Boens, B. Verbelen, W. Dehaen, Postfunctionalization of the BODIPY Core: Synthesis and Spectroscopy, European J. Org. Chem. 2015 (2015) 6577–6595. doi:10.1002/ejoc.201500682.

[29] D. Rognan, The impact of in silico screening in the discovery of novel and safer drug candidates, Pharmacol. Ther. 175 (2017) 47–66.

doi:10.1016/j.pharmthera.2017.02.034.

[30] I.K. Petrushenko, K.B. Petrushenko, Effect of meso-substituents on the electronic transitions of BODIPY dyes: DFT and RI-CC2 study., Spectrochim. Acta. A. Mol. Biomol. Spectrosc. 138 (2015) 623–7. doi:10.1016/j.saa.2014.12.005.

[31] R.R. Valiev, A.N. Sinelnikov, Y.V. Aksenova, R.T. Kuznetsova, M.B. Berezin, A.S. Semeikin, V.N. Cherepanov, The computational and experimental investigations of photophysical and spectroscopic properties of BF2 dipyrromethene complexes, Spectrochim. Acta Part A Mol. Biomol. Spectrosc. 117 (2014) 323–329. doi:10.1016/j.saa.2013.08.042.

[32] M.R. Momeni, A. Brown, Why Do TD-DFT Excitation Energies of BODIPY/Aza-BODIPY Families Largely Deviate from Experiment? Answers from Electron Correlated and Multireference Methods, J. Chem. Theory Comput. 11 (2015) 2619–2632. doi:10.1021/ct500775r.

[33] M. Buyuktemiz, S. Duman, Y. Dede, Luminescence of BODIPY and dipyrrin: An MCSCF comparison of excited states, J. Phys. Chem. A. 117 (2013) 1665–1669. doi:10.1021/jp311939s.

[34] A. Prlj, A. Fabrizio, C. Corminboeuf, Rationalizing fluorescence quenching in meso-BODIPY dyes, Phys. Chem. Chem. Phys. 18 (2016) 32668–32672. doi:10.1039/C6CP06799A.

[35] A. Prlj, L. Vannay, C. Corminboeuf, Fluorescence Quenching in BODIPY Dyes: The Role of Intramolecular Interactions and Charge Transfer, Helv. Chim. Acta. 100 (2017) 1–9. doi:10.1002/hlca.201700093.

[36] P.G. Szalay, T. Muller, G. Gidofalvi, H. Lischka, R. Shepard, Multiconfiguration self-

consistent field and multireference configuration interaction methods and applications, Chem. Rev. 112 (2012) 108–181. doi:10.1021/cr200137a.

[37] O. Christiansen; H. Koch; P. Jørgensen., The second-order approximate coupled cluster singles and doubles model CC2., Chem. Phys. Lett. 243 (1995) 409–418.

[38] A. Dreuw, M. Wormit, The algebraic diagrammatic construction scheme for the polarization propagator for the calculation of excited states, Wiley Interdiscip. Rev. Comput. Mol. Sci. 5 (2015) 82–95. doi:10.1002/wcms.1206.

[39] C. Adamo, D. Jacquemin, The calculations of excited-state properties with Time-Dependent Density Functional Theory, Chem. Soc. Rev. 42 (2013) 845–856. doi:10.1039/C2CS35394F.

[40] A.D. Laurent, C. Adamo, D. Jacquemin, Dye Chemistry with Time-Dependent Density Functional Theory, Phys. Chem. Chem. Phys. 16 (2014) 14334–14356. doi:10.1039/C3CP55336A.

[41] B. Le Guennic, O. Maury, D. Jacquemin, Aza-boron-dipyrromethene dyes: TD-DFT benchmarks, spectral analysis and design of original near-IR structures, Phys. Chem. Chem. Phys. 14 (2012) 157. doi:10.1039/c1cp22396h.

[42] S. Chibani, B. Le Guennic, A. Charaf-Eddin, O. Maury, C. Andraud, D. Jacquemin, On the Computation of Adiabatic Energies in Aza-Boron-Dipyrromethene Dyes, J. Chem. Theory Comput. 8 (2012) 3303–3313. doi:10.1021/ct300618j.

[43] D. Jacquemin, A. Planchat, C. Adamo, B. Mennucci, TD-DFT assessment of functionals for optical 0-0 transitions in solvated dyes, J. Chem. Theory Comput. 8 (2012) 2359–2372. doi:10.1021/ct300326f.

[44] F. Santoro, D. Jacquemin, Going beyond the vertical approximation with time-

dependent density functional theory, Wiley Interdiscip. Rev. Comput. Mol. Sci. 6 (2016) 460–486. doi:10.1002/wcms.1260.

[45] J.J. Nogueira, L. González, Computational Photophysics in the Presence of an Environment, Annu. Rev. Phys. Chem. 69 (2018) 473–97. doi:10.1146/annurev-physchem-050317-021013.

[46] M. Barbatti, K. Sen, Effects of different initial condition samplings on photodynamics and spectrum of pyrrole, Int. J. Quantum Chem. 116 (2016) 762–771. doi:10.1002/qua.25049.

[47] R. Crespo, Q. Mary, M. Barbatti, Spectrum simulation and decomposition with nuclear ensemble : Formal derivation and application to benzene , furan and 2-phenylfuran Spectrum simulation and decomposition with nuclear ensemble : formal derivation and application to benzene , furan and 2-p, Theor Chem Acc. 131 (2012) 1237. doi:10.1007/s00214-012-1237-4.

[48] M. Barbatti, A.J.A. Aquino, H. Lischka, The UV absorption of nucleobases : semi-classical ab initio spectra simulations w, Phys. Chem. Chem. Phys. 12 (2010) 4959–4967. doi:10.1039/c005130f.

[49] M. Cossi, V. Barone, Solvent effect on vertical electronic transitions by the polarizable continuum model, J. Chem. Phys. 112 (2000) 2427. doi:10.1063/1.480808.

[50] M. Cossi, V. Barone, Time-dependent density functional theory for molecules in liquid solutions, J. Chem. Phys. 115 (2001) 4708–4717. doi:10.1063/1.1394921.

[51] M. De Vetta, M.F.S.J. Menger, J.J. Nogueira, L. González, Solvent Effects on Electronically Excited States: QM/Continuum Versus QM/Explicit Models, J. Phys. Chem. B. 122 (2018) 2975–2984. doi:10.1021/acs.jpcb.7b12560.

[52] B. Mennucci, Polarizable continuum model, Wiley Interdiscip. Rev. Comput. Mol. Sci. 2 (2012) 386–404. doi:10.1002/wcms.1086.

[53] A. Klamt, G. Schuurmann, Cosmo - a New Approach To Dielectric Screening in Solvents With Explicit Expressions for the Screening Energy and Its Gradient, J. Chem. Soc. Trans. 2. 5 (1993) 799–805. doi:10.1039/p29930000799.

[54] M.W. Van Der Kamp, A.J. Mulholland, Combined quantum mechanics/molecular mechanics (QM/MM) methods in computational enzymology, Biochemistry. 52 (2013) 2708–2728. doi:10.1021/bi400215w.

[55] H. Lin, D.G. Truhlar, QM/MM: What have we learned, where are we, and where do we go from here?, Theor. Chem. Acc. 117 (2007) 185–199. doi:10.1007/s00214-006-0143-z.

[56] E. a. Briggs, N. a. Besley, D. Robinson, QM/MM excited state molecular dynamics and fluorescence spectroscopy of BODIPY, J. Phys. Chem. A. 117 (2013) 2644–2650. doi:10.1021/jp312229b.

[57] A. D. Becke, A new mixing of Hartree-Fock and local density-functional theories., J. Chem. Phys. 98 (1993) 1372–1377.

[58] P.J.A. Ditchfield R., Hehre, W. J., An Extended Gaussian-Type Basis for Molecular-Orbital Studies of Organic Molecules., J. Chem. Phys. 54 (1971) 724–728.

[59] J.P. Zobel, J.J. Nogueira, L. González, The IPEA dilemma in CASPT2, Chem. Sci. 8 (2017) 1482–1499. doi:10.1039/c6sc03759c.

[60] G. Ghigo, B.O. Roos, P.Å. Malmqvist, A modified definition of the zeroth-order Hamiltonian in multiconfigurational perturbation theory (CASPT2), Chem. Phys. Lett. 396 (2004) 142–149. doi:10.1016/j.cplett.2004.08.032.

[61] B.O. Roos, K. Andersson, Multiconfigurational perturbation theory with level shift — the Cr2 potential revisited, Chem. Phys. Lett. 245 (1995) 215–223. doi:10.1016/0009-2614(95)01010-7.

[62] F. Aquilante, R. Lindh, P. Thomas Bondo, Unbiased auxiliary basis sets for accurate two-electron integral approximations., J. Chem. Phys. (2007) 114107.

[63] D. E. Woon and T. H. Dunning Jr., "Gaussian-basis sets for use in correlated molecular calculations. 3. The atoms aluminum through argon," J. Chem. Phys. 98 (1993) 1358–71.

[64] A. Schäfer, H. Horn, R. Ahlrichs, Fully optimized contracted Gaussian basis sets for atoms Li to Kr, J. Chem. Phys. 97 (1992) 2571–2577. doi:10.1063/1.463096.

[65] C. Adamo, M. Cossi, V. Barone, An accurate density functional method for the study of magnetic properties: the PBE0 model☆, J. Mol. Struct. THEOCHEM. 493 (1999) 145–157. doi:10.1016/S0166-1280(99)00235-3.

[66] T. Yanai, D.P. Tew, N.C. Handy, A new hybrid exchange–correlation functional using the Coulomb-attenuating method (CAM-B3LYP), Chem. Phys. Lett. 393 (2004) 51–57. doi:10.1016/j.cplett.2004.06.011.

[67] J.-D. Chai, M. Head-Gordon, Long-range corrected hybrid density functionals with damped atom–atom dispersion corrections, Phys. Chem. Chem. Phys. 10 (2008) 6615. doi:10.1039/b810189b.

[68] Y. Zhao, D.G. Truhlar, The M06 suite of density functionals for main group thermochemistry, thermochemical kinetics, noncovalent interactions, excited states, and transition elements: two new functionals and systematic testing of four M06-class functionals and 12 other function, Theor. Chem. Acc. 120 (2008) 215–241.

doi:10.1007/s00214-007-0310-x.

[69] F. Plasser, S.A. Bäppler, M. Wormit, A. Dreuw, New tools for the systematic analysis and visualization of electronic excitations. II. Applications, J. Chem. Phys. 141 (2014) 24107. doi:10.1063/1.4885820.

[70] Jmol: an open-source Java viewer for chemical structures in 3D.

[71] R.L. Martin, Natural transition orbitals, J. Chem. Phys. 118 (2003) 4775–4777. doi:10.1063/1.1558471.

[72] F. Plasser, M. Wormit, A. Dreuw, New tools for the systematic analysis and visualization of electronic excitations. I. Formalism, J. Chem. Phys. 141 (2014). doi:10.1063/1.4885819.

[73] A. Schafer, A. Klamt, D. Sattel, J.C.W. Lohrenz, F. Eckert, COSMO Implementation in TURBOMOLE : Extension of an efficient quantum chemical code towards liquid systems COSMO-Implementation in TURBOMOLE : Extension of an efficient quantum chemical code towards liquid systems, Phys. Chem. Chem. Phys. 2 (2000) 2187–2193. doi:10.1039/b000184h.

[74] C. Hättig, F. Weigend, CC2 excitation energy calculations on large molecules using the resolution of the identity approximation, J. Chem. Phys. 113 (2000) 5154–5161. doi:10.1063/1.1290013.

[75] B.M. M. J. Frisch, G. W. Trucks, H. B. Schlegel, G. E. Scuseria, M. A. Robb, J. R. Cheeseman, G. Scalmani, V. Barone, G. A. Petersson, H. Nakatsuji, X. Li, M. Caricato, A. Marenich, J. Bloino, B. G. Janesko, R. Gomperts, Gaussian 09, Revision A.02.

[76] F. Furche, R. Ahlrichs, C. Hättig, W. Klopper, M. Sierka, F. Weigend, Turbomole,

Wiley Interdiscip. Rev. Comput. Mol. Sci. 4 (2014) 91–100. doi:10.1002/wcms.1162.

[77] R.L. F. Aquilante, L. De Vico, N. Ferré, G. Ghigo, P.-Å. Malmqvist, P. Neogrády, T. B. Pedersen, M. Pitonak, M. Reiher, B. O. Roos, L. Serrano-Andrés, M. Urban, V. Veryazov, MOLCAS 7, J. Comput. Chem. 31 (2010) 224.

[78] S. Chibani, A.D. Laurent, B. Le Guennic, D. Jacquemin, Improving the Accuracy of Excited-State Simulations of BODIPY and Aza-BODIPY Dyes with a Joint SOS-CIS(D) and TD-DFT Approach, J. Chem. Theory Comput. 10 (2014) 4574–4582. doi:10.1021/ct500655k.

[79] M. Laine, N.A. Barbosa, R. Wieczorek, M.Y. Melnikov, A. Filarowski, Calculations of BODIPY dyes in the ground and excited states using the M06-2X and PBE0 functionals, J. Mol. Model. 22 (2016) 260. doi:10.1007/s00894-016-3108-8.

[80] biolitec research GmbH, Private communication.

[81] S. Kümmel, Charge-Transfer Excitations: A Challenge for Time-Dependent Density Functional Theory That Has Been Met, Adv. Energy Mater. 7 (2017) 1–6. doi:10.1002/aenm.201700440.

[82] M.A. Rohrdanz, K.M. Martins, J.M. Herbert, A long-range-corrected density functional that performs well for both ground-state properties and time-dependent density functional theory excitation energies, including charge-transfer excited states, J. Chem. Phys. 130 (2009) 1–8. doi:10.1063/1.3073302.

[83] M.A. Mosquera, A. Wasserman, Derivative discontinuities in density functional theory, Mol. Phys. 112 (2014) 2997–3013. doi:10.1080/00268976.2014.968650.

[84] M. De Vetta, L. González, I. Corral Perez, The role of electronic triplets and high-lying singlet states in the deactivation mechanism of the parent BODIPY: an ADC(2)

and CASPT2 study., ChemPhotoChem. (2018). doi:10.1002/cptc.201800169.

[85] H. Kang, Y. Si, J. Liu, L. Chen, Y. Li, H. Chen, J. Groeper, B. Yang, An experimental and theoretical study of dimethylaminostyryl BODIPY-perylenetetracarboxylic derivative dyads: synthesis, properties and DFT calculation, RSC Adv. 6 (2016) 23094–23101. doi:10.1039/C5RA25139G.

[86] L. Jiao, C. Yu, J. Wang, E.A. Briggs, N.A. Besley, D. Robinson, M.J. Ruedas-Rama, A. Orte, L. Crovetto, E.M. Talavera, J.M. Alvarez-Pez, M. Van der Auweraer, N. Boens, Unusual spectroscopic and photophysical properties of meso-tert-butylBODIPY in comparison to related alkylated BODIPY dyes, RSC Adv. 5 (2015) 89375–89388. doi:10.1039/C5RA17419H.

[87] A. Orte, E. Debroye, M.J. Ruedas-Rama, E. Garcia-Fernandez, D. Robinson, L. Crovetto, E.M. Talavera, J.M. Alvarez-Pez, V. Leen, B. Verbelen, L. Cunha Dias de Rezende, W. Dehaen, J. Hofkens, M. Van der Auweraer, N. Boens, Effect of the substitution position (2, 3 or 8) on the spectroscopic and photophysical properties of BODIPY dyes with a phenyl, styryl or phenylethynyl group, RSC Adv. 6 (2016) 102899–102913. doi:10.1039/C6RA22340K.

[88] T.N. Singh-rachford, A. Haefele, R. Ziessel, F.N. Castellano, Boron Dipyrromethene Chromophores : Next Generation Triplet Acceptors / Annihilators for Low Power Upconversion Schemes Boron Dipyrromethene Chromophores : Next Generation Triplet Acceptors / Annihilators for Low Power Upconversion Schemes, J. Am. Chem. Soc. 130 (2008) 16164–16165. doi:10.1021/ja807056a.

[89] P. Yang, J. Zhao, W. Wu, X. Yu, Y. Liu, Accessing the Long-Lived Triplet Excited States in Bodipy- Conjugated 2- (2-Hydroxyphenyl) Benzothiazole / Benzoxazoles and Applications as Organic Triplet Photosensitizers for Photooxidations, J. Org.

Chem. 77 (2012) 6166–6178.

[90] X.-F. Zhang, X. Yang, K. Niu, H. Geng, Phosphorescence of BODIPY dyes, J. Photochem. Photobiol. A Chem. 285 (2014) 16–20. doi:10.1016/j.jphotochem.2014.04.009.

[91] W. Wu, H. Guo, W. Wu, S. Ji, J. Zhao, Organic triplet sensitizer library derived from a single chromophore (BODIPY) with long-lived triplet excited state for triplet-triplet annihilation based upconversion, J. Org. Chem. 76 (2011) 7056–7064. doi:10.1021/jo200990y.

[92] C. Zhang, J. Zhao, Triplet excited state of diiodoBOPHY derivatives: preparation, study of photophysical properties and application in triplet-triplet annihilation upconversion, J. Mater. Chem. C. 4 (2016) 1623–1632. doi:10.1039/C5TC03193A.

[93] C. Zhang, J. Zhao, X. Cui, X. Wu, Thiol-Activated Triplet–Triplet Annihilation Upconversion: Study of the Different Quenching Effect of Electron Acceptor on the Singlet and Triplet Excited States of Bodipy, J. Org. Chem. 80 (2015) 5674–5686. doi:10.1021/acs.joc.5b00557.

[94] M.A. El-Sayed, Spin—Orbit Coupling and the Radiationless Processes in Nitrogen Heterocyclics, J. Chem. Phys. 38 (1963) 2834. doi:10.1063/1.1733610.

[95] N. Epelde-Elezcano, V. Martínez-Martínez, E. Peña-Cabrera, C.F.A. Gómez-Durán, I.L. Arbeloa, S. Lacombe, Modulation of singlet oxygen generation in halogenated BODIPY dyes by substitution at their meso position: towards a solvent-independent standard in the vis region, RSC Adv. 6 (2016) 41991–41998. doi:10.1039/C6RA05820E.